

Ultrasonic Spectroscopic Evaluation of the Ring-Opening Metathesis Polymerization of Dicyclopentadiene

GREGORY S. CONSTABLE, ALAN J. LESSER, E. BRYAN COUGHLIN

Polymer Science and Engineering Department, University of Massachusetts, Amherst, Massachusetts 01003

Received 18 March 2002; revised 27 January 2003; accepted 28 January 2003

ABSTRACT: An *in situ* ultrasonic spectroscopy technique was used to study the ring-opening metathesis polymerization of dicyclopentadiene catalyzed by bis(tricyclohexylphosphine)benzylidene ruthenium dichloride. A reaction cell employing a flexible poly(ethylene terephthalate) window for pulse echo ultrasonic spectroscopy was used to monitor the polymerization. The changes in the density, wave speed, acoustic modulus, and attenuation were all simultaneously monitored. In comparison with Fourier transform infrared (FTIR) spectroscopy data, the changes in the density, velocity, and modulus only accurately measured the rate constant for the metathesis of the cyclopentyl unsaturation. The ultrasonic values were within 6% of the values determined by FTIR. The activation energy for metathesis of the cyclopentyl unsaturation was 84 kJ mol⁻¹, following first-order kinetics. Rate constants for the polymerization of the norbornyl unsaturation could not be determined by ultrasound. The gel point, vitrification, and qualitative information about the reaction rate could be determined from the change in the attenuation. © 2003 Wiley Periodicals, Inc. *J Polym Sci Part B: Polym Phys* 41: 1323–1333, 2003

Keywords: dicyclopentadiene; ultrasonic spectroscopy; ring-opening metathesis polymerization; crosslinking; kinetics; thermoset

INTRODUCTION

Poly(dicyclopentadiene) (PDCPD) is a commercially important thermoset polymer because of its high modulus, impact strength, and chemical resistance.¹ PDCPD is attractive not only for its physical and mechanical properties but also for its ease of fabrication. The polymerization of dicyclopentadiene (DCPD) with metathesis catalysts is performed with reaction injection molding (RIM) to manufacture snowmobile and boat housings, chlorine cell covers, and wastewater treatment equipment.² The chemistry of DCPD ring-

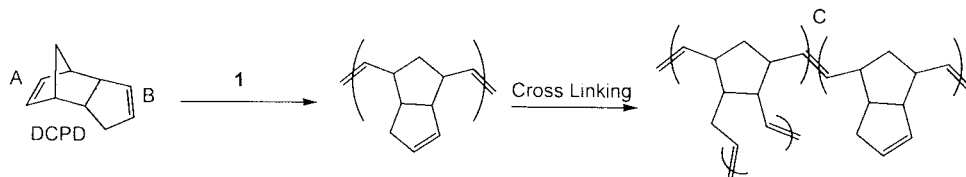
opening metathesis polymerization (ROMP) forms a crosslinked article in a matter of minutes, at which point it can be removed from the mold and postcured.³

Although the reaction rate and crosslinking of DCPD are ideal for RIM systems, the conversion characterization can be nontrivial. Common solution methods of polymer analysis, such as size exclusion chromatography, are not possible. One commonly used method for monitoring the cure of thermosets is differential scanning calorimetry (DSC).^{4,5} Yang et al.⁶ used DSC to study the curing of polyester resins by correlating the accumulated exotherm to the conversion and reaction rate. There are, however, a number of limitations to this technique. The heat capacity, density, and heat of reaction must remain constant during the reaction, and the heats of reaction for all the reactions must be equal. The ROMP of DCPD

Correspondence to: (regarding ultrasound) A. J. Lesser (E-mail: ajl@polysci.umass.edu)

Correspondence to: (regarding chemistry) E. B. Coughlin (E-mail: coughlin@mail.pse.umass.edu)

Journal of Polymer Science: Part B: Polymer Physics, Vol. 41, 1323–1333 (2003)
© 2003 Wiley Periodicals, Inc.



Scheme 1. Reaction mechanism for the polymerization of DCPD.

does not satisfy these assumptions. First, the density increases from 0.977 to 1.03 g/cm³ with the conversion to the polymer. Also, the initial polymerization of DCPD occurs through the more strained norbornyl double bond (A, Scheme 1), whereas crosslinking occurs at a slower rate through the less strained cyclopentyl double bond (B, Scheme 1). A third possible reaction in the ROMP of DCPD is cross metathesis with unsaturations in the polymer chains, contributing slightly to the overall heat of reaction, but not to conversion. Such errors would lead to an underestimation of the degree of conversion.

Yang et al.⁷ used ¹H NMR to confirm that DSC measurements underestimated the degree of conversion of DCPD, but they were not able to quantify the value. Their experiments on the bulk polymerization of DCPD demonstrated that conversion could be followed by solution ¹H NMR. Because only mobile molecules are observed in solution NMR, residual monomer in the PDCPD network was qualitatively measured. Quantitative measurements of conversion could not be attained without the use of an internal standard. Even if a standard was employed, solution NMR was not fast enough to monitor high reaction rates with good signal-to-noise ratios. NMR spectra in this experiment were only collected at the gel point and twice more during cure. Solid-state ¹³C cross-polarization/magic-angle spinning NMR of curing PDCPD was also studied.⁸ Once again, this method is limited by the scan time and signal-to-noise ratio. More importantly, shifts in the ¹³C spectra on conversion from DCPD to PDCPD are not significant enough for a change to be observed in the spectrum.

Ultrasonic spectroscopy has been used to monitor thermoset polymerizations. Lindrose⁹ used ultrasound to study the curing of epoxies. Pulse echo scans from longitudinal and shear transducers were used to measure the apparent longitudinal, shear, Young's, and bulk modulus changes in a curing epoxy. In this setup, the transducers were connected to a coaxial switcher and mounted to the base plate on which an epoxy was cured.

This allowed almost simultaneous signal processing from both transducers. From an analysis of the pulse echo data sets, Lindrose was able to deduce that the bulk modulus of the curing epoxy varied as a function of time, and there was synchronous behavior between the bulk and shear moduli.

Recently, the curing of an epoxy was studied by DSC, dynamic mechanical analysis (DMA), and ultrasound to compare and contrast the utility of each technique to monitor the curing of an epoxy.¹⁰ In the study, the degree of cure was analyzed by the monitoring of the heat of reaction by isothermal DSC, the complex modulus by DMA, and the longitudinal velocity by ultrasound. The analysis showed that once DSC reached a maximum in the degree of cure, there was still a significant increase in the longitudinal velocity and, therefore, network formation, except at higher temperatures. It was concluded that although DSC offered no information on cure after vitrification and DMA could not practically be used until gelation, ultrasound was ideal because it was sensitive over the range of cure states.

Alig et al.¹¹ used pulse transmission ultrasonic spectroscopy to monitor velocity and attenuation changes during the cure of an epoxy. From the data, changes in the real and imaginary portions of the longitudinal modulus were calculated to determine structural relaxation times. It was found that in some cases the gel time could be determined from a plateau region in the real and imaginary portions of the longitudinal modulus. Ultrasonic gel times were in good agreement with DMA, Brillouin light scattering, and dielectric measurements.

Schueneman¹² used through transmission ultrasonic spectroscopy to monitor the curing of epoxy and rubber-modified epoxy. As the sound velocity of the curing epoxy increased sharply, the attenuation coefficient reached a peak value. This phenomenon was attributed to the increase in the modulus with the vitrification of the epoxy. Younes et al.¹³ drew a similar conclusion for curing epoxies. It was determined that the gel point,

as measured by viscometry, occurred before the maximum in the attenuation, and it was attributed to vitrification

In this work, a reaction cell was constructed with a flexible poly(ethylene terephthalate) (PET) window for use in pulse echo ultrasonic spectroscopy to monitor the cure and densification of DCPD as it underwent ROMP. The density, longitudinal velocity, acoustic modulus, and attenuation were monitored with respect to the reaction time.

EXPERIMENTAL

Materials

The metathesis catalyst, bis(tricyclohexylphosphine)benzylidene ruthenium dichloride (**1**), was purchased from Strem Chemical. All other reagents were purchased from Aldrich and used as received unless otherwise noted. DCPD was melted and purified by passage through warm activated basic alumina before use. For DCPD polymerizations, stock solutions of **1** and triphenylphosphine (PPh_3) in dry and degassed benzene were prepared and kept frozen until needed. DCPD, **1**, and PPh_3 solutions were measured at molar ratios of 7500/15,000/22,500 equiv of DCPD or DCPD/tricyclo[5.2.1.0]dec-8-ene (TCD) solution to 2 mol equiv of PPh_3 to 1 mol equiv of **1**. The reactants were mixed in a vial and then injected into the reaction cell via a syringe. The reactions were run at 25, 35, 50, and 65 °C.

TCD was prepared according to a literature procedure,¹⁴ and the reaction intermediates and final product were characterized by NMR and gas chromatography/mass spectrometry (GC-MS). ^1H and ^{13}C NMR spectra were recorded on a Bruker DPX 300-MHz instrument, and GC-MS spectra were recorded on an HP 5890 series II gas chromatograph with an HP 5989A mass spectrometer. For a comparison of ultrasonic spectroscopy to Fourier transform infrared (FTIR), solutions of DCPD and 10 wt % TCD were polymerized at 25 °C and monitored by each technique.

FTIR Spectroscopy

FTIR spectra were collected as thin films on NaCl plates with a Bio-Rad FTS 1752 FTIR spectrometer. Four scans were collected and averaged per data point. Scans were collected every 15 min for an 18-h period. Spectra were analyzed with Bio-

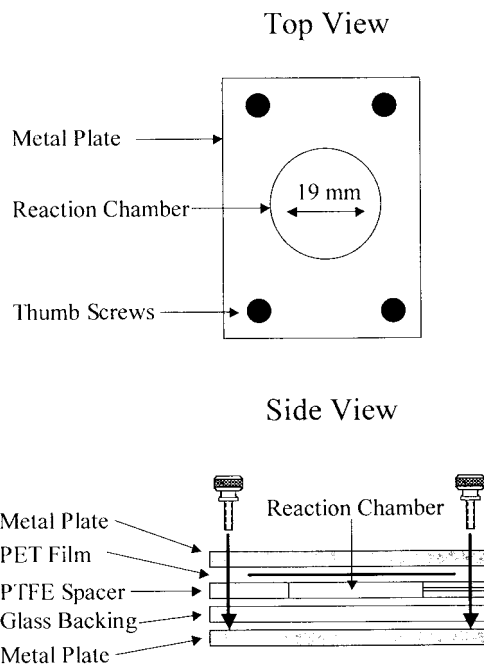


Figure 1. Ultrasound reaction cell for DCPD polymerizations.

Rad Win-IR software. The data were analyzed by the monitoring of the evolution of the 975-cm^{-1} carbon hydrogen bending vibration of a trans carbon double bond as a function of time.¹⁵ This vibration was well separated from other vibrations and did not require deconvolution. Additionally, the DCPD/TCD monomer solution only contained cis double bonds, and ROMP by **1** primarily produced trans double bonds (90% trans);¹⁶ Therefore, this peak was ideal for monitoring the extent of polymerization.

Reaction Cell Design

Figure 1 depicts the structure of the reaction cell. It consisted of two machined metal plates, 3-mm-thick plate glass backing, a 3-mm poly(tetrafluoroethylene) (PTFE) spacer, 50- μm PET film, and four thumbscrews. The reaction chamber was 19 mm in diameter and 3 mm thick. The thickness was chosen for ease in charging the cell and the setup of the ultrasound instrumentation. Plate glass was chosen as the back surface of the reaction chamber for its smoothness, inertness, and high reflection coefficient. PET was chosen as the cover because it was inert to the chemistry and conditions involved in this study and its impedance value closely matched that of water and the

reactants. The PET film was thin enough that only one reflection from the film was observed. More importantly, the PET film was flexible enough to contract with the sample as the polymerization progressed. This allowed for accurate instantaneous measurements of the sample thickness, and therefore, the density. The reactants were introduced into the reaction chamber via a syringe inserted through a small hole in the PTFE spacer. Once the reactants were injected, the hole was filled with inert high-vacuum silicone grease (Dow Corning) so that inertness would be maintained. Because **1** was chemically robust, anhydrous and anaerobic conditions were not necessary for high conversions to be achieved, and this simplified the sample preparation.¹⁷

Ultrasonic Spectroscopy

A Panametrics model 5900 200-MHz pulser/receiver digitized with a Sonix 1-GHz STR81G PC digitizer was used in this study. The pulser/receiver was digitized at a rate of 1 GHz to drive the 10-, 20-, 30-, and 50-MHz transducers. The transducers used were the following Panametrics models: a V312 10-MHz focused transducer with a 25.4-mm focal length, a V316 20-MHz focused transducer with a 19-mm focal length, a V375 30-MHz focused transducer with a 19-mm focal length, and a V390 50-MHz focused transducer with a 12.7-mm focal length. For an experiment to be started, the reaction cell, already containing the activated catalyst and monomer, was placed horizontally in a jacketed water bath with pure water as the coupling medium. The transducer was lowered into the water bath, via a jig, and focused on the PET cover of the reaction cell. Focus was achieved by the adjustment of the distance between the transducer and the reaction cell until the amplitude of the reflection through the reaction cell (t_2 ; Fig. 2) was maximized. The temperature of the water bath was regulated with a VWR Scientific model 1157 circulator with a programmable temperature controller. Panametrics Multiscan software was used to gate and analyze the waveforms. Five waveforms were collected and averaged at specific intervals over the course of the reaction.

Calculation of the Ultrasound Parameters

Pulse echo ultrasonic spectroscopy measures the elapsed time for a sound wave to travel twice through a medium and reflect back to the trans-

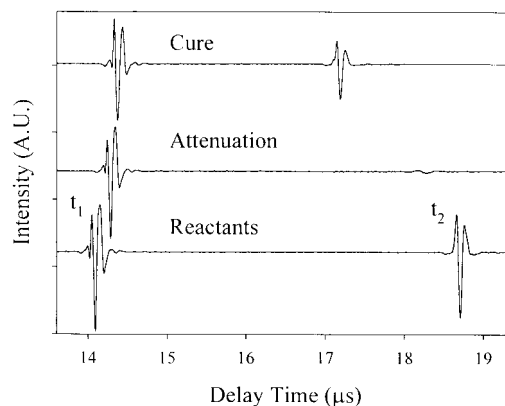


Figure 2. Pulse echo waveforms at initiation, near vitrification, and at the final cure of DCPD polymerization with a 20-MHz transducer. The change in the delay time for the reflection off the PET film (t_1) is due to densification, and the change in the delay time of the reflection off the glass backing (t_2) is due to the increase in the sound velocity.

ducer. If the distance the wave has traveled is known, the velocity of sound in that medium can be calculated. The velocity (C_L) of sound through the medium is dependent on the modulus (E) and density (ρ) of the medium:

$$E \approx \rho C_L^2 \quad (1)$$

In this setup, which takes advantage of this relationship, both the velocity and density are measured independently from a single waveform. A typical pulse echo waveform of sound that has traveled through the reaction cell is displayed in Figure 2. The more intense reflection, t_1 , is the reflection off the PET film. The less intense reflection, t_2 , is the reflection off the glass backing and represents a sound wave that has traveled through the sample and has been reflected back to the transducer. By turning off the trigger and gating a fixed area around the reaction cell waveforms, we can monitor the changes in the delay times of the maximum amplitude of reflections t_1 and t_2 . Reflection t_1 moves to longer delay times because of densification of the medium. This change can be observed because the reaction cell holds the polymer in a plane strain geometry, causing the shrinkage to occur strictly from the top, that is, the PET interface. The sample thickness, h , was calculated as follows:

$$h = h_f + \frac{C_{Lw}(t_{1o} - t_1)}{2} \quad (2)$$

where h_f is the final thickness of the sample as measured by calipers, C_{LW} is the longitudinal velocity of sound in water, and t_{10} is the delay time of the reflection off the PET film at the start of the reaction. The sample density (ρ) was calculated by the removal of a cylindrical volume from the center of the cured polymer sample. The mass, final thickness, and diameter were measured externally, from which the instantaneous thickness, volume, and density were calculated. The final product densities were compared with those measured according to ASTM D 792 in 22 °C deionized water.

The extent of the reaction is assumed to correlate with the decrease in the delay time of the reflection off the glass plate. Because the glass plate is fixed with respect to the transducer, the decrease in the delay time is due to an increase in the sound velocity. C_L can then be calculated as follows:

$$C_L = \left(\frac{2h}{t_2 - t_1} \right) \quad (3)$$

Full attenuation of reflection t_2 is observed for a period of time during the reaction because of absorption of the ultrasonic energy by the viscoelastic nature of the reactant. This phenomenon has been observed in epoxies and has been related to the gelation and vitrification of the polymer.^{13,18} The reduced attenuation (eq 4) was derived in a fashion similar to that of Lee et al.:¹⁹

$$\alpha = h \ln\left(\frac{Y}{R}\right) \quad (4)$$

$$\alpha = \frac{\alpha_0}{\alpha_t} \quad h = \frac{h_0}{h_t} \quad Y = \frac{Y_0}{Y_t} \quad R = \frac{R_0}{R_t} \quad (5)$$

$$R = (1 - R_1^2)R_2 \quad (6)$$

where α , h , Y , and R are the ratios of the attenuation, thickness, frequency transform function, and reflection coefficient at time zero and at time t (eq 5). The ratio of the reflection coefficient accounts for the scattered energy at the PET–sample interface (R_1) and the sample–glass interface (R_2 ; eq 6).

Calculation of the Rate Constants

The observed rate constant for the ROMP of DCPD is the compilation of three distinct chemi-

cal reactions: the activation of **1**, the metathesis of the norbornyl double bond (bond A, Scheme 1), and the metathesis of the cyclopentyl double bond (bond B). The activation of **1** occurs by dissociation of a tricyclohexylphosphine ligand and coordination of the monomer, which is reversible until the monomer reacts by forming the propagating alkylidene.^{20,21} The equilibrium between the coordinated phosphine and monomer can be shifted toward the inactive catalyst by the addition of more phosphine, which, in turn, lowers the reaction rate. To increase the time to gelation, we added 2 mol equiv of PPh_3 to push the equilibrium toward the inactive catalyst,²² allowing the monomer and catalyst to be mixed externally and then to be injected into the reaction cell. The formation of the polymer network initially occurs through polymerization of the unsaturation in the more strained norbornyl ring, forming linear PDCPD, with subsequent crosslinking through the less strained cyclopentyl ring.²³

The activation of **1** is assumed to be at a steady state throughout the reaction and will not be further discussed. Polymerization kinetics, as monitored by FTIR and ultrasound, are viewed as two parallel first-order reactions producing a common product. Specifically, the metathesis of A, with a rate constant k_1 , producing a trans double bond (bond C) with an IR absorption at 975 cm^{-1} , and the metathesis of B, with a rate constant k_2 , producing an IR equivalent trans double bond. A rate equation can be derived for the formation of C:

$$C = C_\infty - A_0 e^{-k_1 t} - B_0 e^{-k_2 t} \quad (7)$$

where C_∞ is the final concentration of the product, A_0 and B_0 are the initial concentrations of bonds A and B, and t is the reaction time. FTIR and ultrasound data were normalized by eq 8, and this resulted in $C_0 = 0$ and $C_\infty = 1$. Fitting eq 7 to the data allowed the rate constants to be directly calculated and compared:

$$C = \frac{(C - C_i)}{(C_f - C_i)} \quad (8)$$

RESULTS AND DISCUSSION

Density

To verify that the pulse echo ultrasound and the reaction cell design were reliable for monitoring changes in the density, we compared the initial

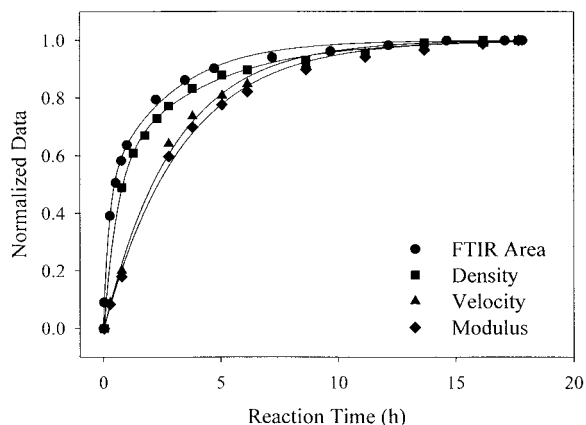


Figure 3. Rate of conversion of 15,000 mol of DCPD/TCD polymerized at 25 °C as measured by IR and 20-MHz ultrasound. The solid lines through the FTIR and density data are fits of eq 7, whereas the velocity and modulus are fits of eq 9.

and final densities of DCPD. The density of DCPD at 35°C was measured to be 0.960 g/cm³ with an actual density of 0.977 g/cm³.²⁴ The product density was calculated to be 1.030 g/cm³ with an actual value of 1.033 g/cm³. Over the entire reaction time, the densities measured by ultrasound were in agreement with those measured by ASTM D 792. The ultrasonic values had less than 1% error, which could be attributed to small differences in the temperature and the assumption that the sample had an ideal cylindrical geometry. The agreement of these values verifies that during polymerization, the densification change can accurately be monitored by this technique.

Monomer Concentration

To evaluate ultrasonic spectroscopy as a technique for monitoring conversion during polymerization, we compared the rate of change in the density, sound velocity, and acoustic modulus of the ROMP of DCPD/TCD solutions to data obtained by FTIR. The reaction rates measured by ultrasonic spectroscopy were lower than those measured by FTIR. This is depicted in Figure 3, which shows normalized FTIR and ultrasound data for the polymerization of 15,000 mol equiv of DCPD/TCD. The rate of densification closely corresponded to the rate of conversion as measured by FTIR. Throughout the polymerization, densification occurred at a rate comparable to, but slightly lower than, the rate of ROMP of both the norbornyl and cyclopentyl unsaturations. In com-

parison, the conversion percentages measured by sound velocity and acoustic moduli were always lower than those measured by FTIR and density, with the modulus being slightly lower than velocity. Similar trends were observed in reactions with different monomer concentrations. As the monomer concentration increased, the rate of conversion decreased, as depicted in Figure 4 by the change in the sound velocity with respect to the reaction time and monomer concentration. This trend was confirmed by FTIR analysis. Matusukawa and Nagai²⁵ clearly showed, for the curing of epoxies with different concentrations of the curing agent, that the rate of the change of the sound velocity increased with an increasing reaction rate.

To quantify these observations, we fit eq 7 to the data, and the rate constants k_1 and k_2 were extracted. The rate constants k_1 and k_2 for the polymerization of 15,000 mol of DCPD/TCD, determined by FTIR, were 4.11 and 0.3594 h⁻¹, respectively. Various monomer concentrations revealed that k_1 and k_2 decreased with an increasing monomer concentration (Fig. 5). The measurement of k_1 by the rate of densification was approximately 35% lower than k_1 , as determined by FTIR. The trend of decreasing k_1 with an increasing monomer concentration was observed in both cases. From observations of Figure 3, we concluded that the rate of densification closely corresponded to the rate of reaction of both unsaturations. A more accurate analysis from the calculation of the rate constants clearly showed that densification was affected more by the crosslinking reaction, k_2 , than the linear polymerization, k_1 . Therefore, the rate of densification corre-

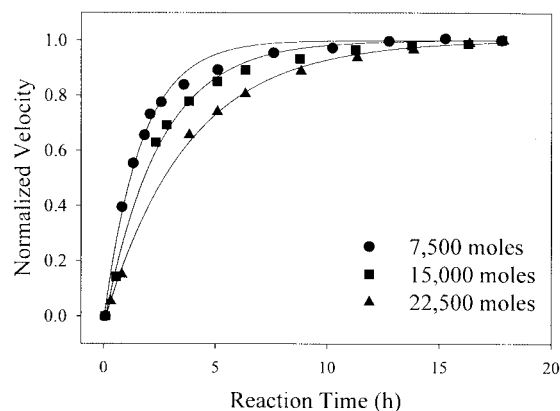


Figure 4. Change in the normalized velocity as a function of the monomer concentration for the polymerization of DCPD/TCD fitted with eq 9 (solid lines).

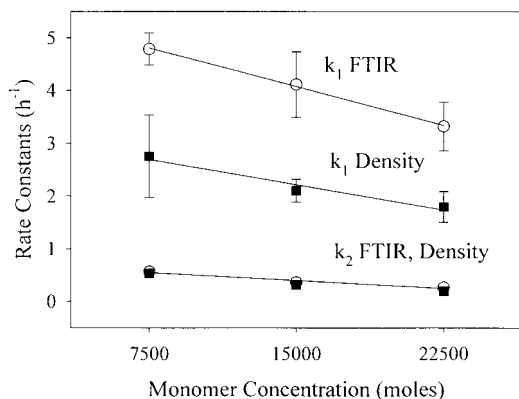


Figure 5. Comparison of rate constants k_1 and k_2 as measured by (○) FTIR and (■) density data with a linear fit through the data set. The error bars are the standard errors for the coefficient. There is negligible error for the k_2 values.

sponded qualitatively to k_1 but quantitatively to k_2 .

Equation 7 cannot accurately be fit to the velocity and modulus data. This difference can be explained if we realize that each technique measures a different property of the system. FTIR spectroscopy monitors the relative concentration of a particular functional group, whereas ultrasound monitors the physical and mechanical properties of the material, which may or may not change with the concentration. Because the mechanical properties of the polymer were greatly changed on crosslinking, it can be assumed that the changes in the velocity and modulus were more affected by the crosslinking reaction, k_2 , than the linear polymerization, k_1 . This was observed in the data as the lower slope of the velocity and modulus curves with respect to FTIR (Fig. 3). With this in mind, we removed the $A_0 e^{-k_1 t}$ term from eq 7 to yield eq 9 and applied it to the velocity and modulus data:

$$C = C_\infty - B_0 e^{-k_2 t} \quad (9)$$

Figure 6 shows the rate constant k_2 , determined by eq 9, for each technique at various monomer concentrations. The k_2 values measured from ultrasound were within 3% of that measured by FTIR. Although the fits of eq 9 to the velocity and modulus data deviated at higher conversions, a log plot of the velocity versus the reaction time was linear for approximately three half-lives, validating this first-order fit. By realizing the differences in the properties measured by each tech-

nique and appropriately modifying eq 7, we could attain an accurate value for k_2 from the ultrasonic data.

To verify that the attenuation did not affect the calculated rate constants, we ran comparative reactions over a range of transducer frequencies. Although the waveforms were well separated, even at the minimum sample thickness (2 mm) that allowed for the injection of the reactions, a similar duration of attenuation was observed. Therefore, it was necessary to reduce the transducer frequency. Compared with the higher frequency transducers, 10 MHz did not fully attenuate during the reaction (Fig. 7). The 10-MHz data set shows that there was an inflection point at the onset of full attenuation, which was not apparent at higher frequencies. The rate equations, 7 and 9, do not accurately model this behavior. However, the calculation of k_2 by eq 9 revealed that there was only a 2.75% change in the rate constant and a small decrease in the R^2 value in comparison with the 20-MHz data. At 30 and 50 MHz, there was a larger decrease in k_2 due to the increased duration of full attenuation. The attenuation behavior with respect to the transducer frequency can be observed later in Figure 12 and is addressed shortly. Therefore, it is concluded that the attenuation of the 20-MHz data did not affect the calculated rate constants.

The reaction rate was also analyzed with respect to the attenuation spectra. The change in the reduced attenuation coefficient for the polymerization of DCPD/TCD is shown in Figure 8. The attenuation coefficient underwent an initial sharp increase during the first hour of reaction to a point at which the sound wave was fully ab-

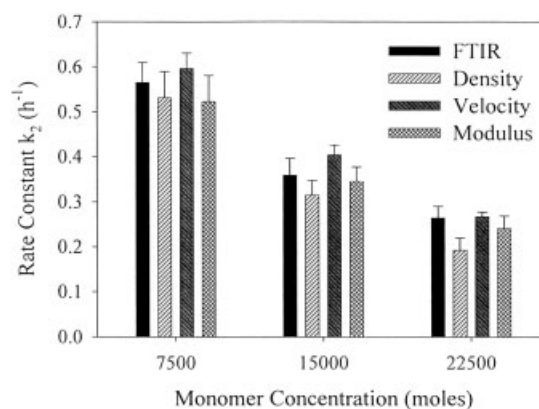


Figure 6. Comparison of the k_2 rate constant determined by the fitting of the FTIR and density to eq 7 and the velocity and modulus to eq 9.

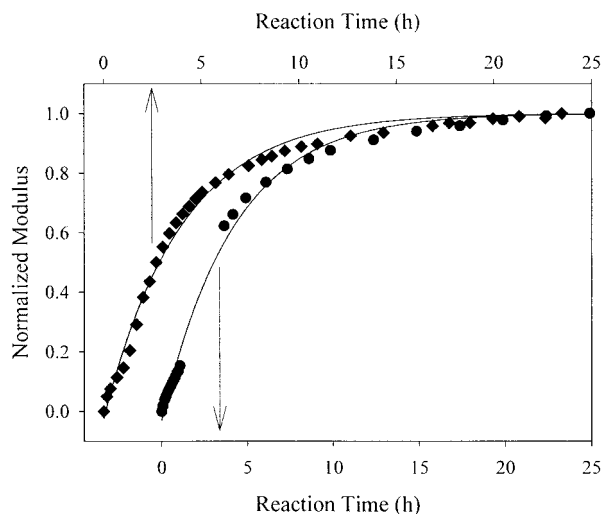


Figure 7. Modulus data for the polymerization of DCPD at 35°C collected with 10- and 20-MHz transducers. The ordinate has been shifted to separate the overlapping data.

sorbed by the media. The period of full attenuation was followed by a gradual decrease in attenuation as the polymer cured. As the monomer concentration increased, the curve shifted to longer reaction times and the peak broadened. This phenomenon was also observed by Freemantle and Challis²⁶ and Matsukawa and Nagai²⁵ during the cure of the epoxy resins. They determined that the width and position of the attenuation peak were related to the reaction rate and extent of crosslinking. As the reaction rate increased, the attenuation peak narrowed and shifted to shorter reaction times. Figure 8 illustrates that a change in the reaction rate was observable as verified by the concentration dependence determined from the FTIR and ultrasound analysis. The time of initial recovery of the t_2 signal occurred at approximately 1.8, 2.8, and 3.8 h in order of increasing monomer concentration. For all three reactions, the velocity and modulus at which the signal returns were approximately 1880 m/s and 3.5 GPa. Only approximate values could be attained because of the low signal-to-noise ratio at such small signal amplitudes. Therefore, the polymer needs to reach a level of cure, characterized by the modulus and velocity values, before the signal returned. The quantitative degree of conversion and reaction rate could not be determined from the attenuation spectra.

Viscoelastic information could be extracted from the attenuation coefficient. Within 20 min of

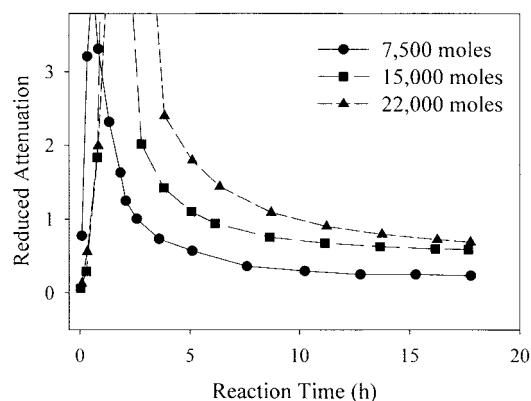


Figure 8. Reduced attenuation coefficient during the polymerization of DCPD/TCD.

catalyst **1** and PPh_3 being mixed with the monomer, a soft and rubbery insoluble plug was formed. The sample maintained this character and slowly stiffened as it cured through the attenuation peak. After full attenuation, it continued to cure to a glass. Woodson and Grubbs²² showed that the gel point for pure DCPD under similar conditions occurred in 11 min. Therefore, it is believed that gelation occurs near the onset of attenuation with vitrification occurring at the peak in attenuation. The reaction is then diffusion-controlled, and this leads to the longer curing times.

The rate of polymerization of bulk DCPD was also studied by ultrasound. The increase in the velocity as a function of the reaction time is depicted in Figure 9. All three-concentration curves

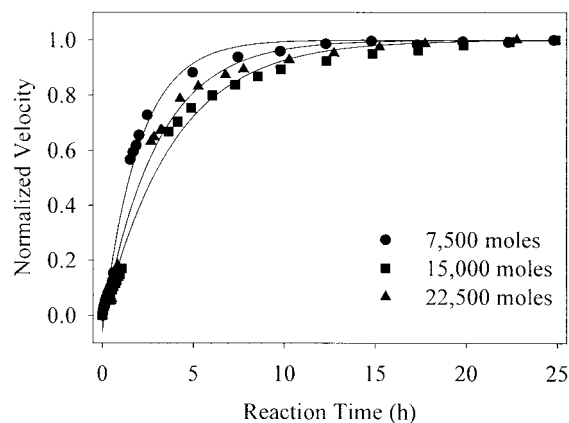


Figure 9. Change in the velocity during the polymerization of DCPD as a function of the monomer concentration at 35°C. The solid lines are the regressions of eq 9.

followed approximately the same exponential curve, with a maximum value after approximately 10 h of cure at 35 °C. The k_2 values were 0.501 h^{-1} for 7500 mol, 0.262 h^{-1} for 15,000 mol, and 0.331 h^{-1} for 22,500 mol DCPD. Bulk DCPD did not exhibit the rate dependence on the monomer concentration, as did the DCPD/TCD solution. This could be caused by either the increase in the reaction temperature (from 25 to 35 °C to melt DCPD) or the added TCD. The temperature change could raise the reaction rate such that the reaction became diffusion-controlled before a rate dependence could be monitored. In comparison, the added TCD lacked functionality for crosslinking, decreasing the crosslink density and, therefore, changing the time to vitrification. This allowed more time for us to observe the reaction rate before the polymerization became diffusion-controlled. In comparison to the DCPD/TCD reactions, the signal for all the monomer concentrations was recovered at approximately 3 h. Because all the reactions reached a similar sound velocity (1900 m/s) and modulus (3.6 GPa) at recovery from full attenuation, vitrification had to occur at a definite crosslink density. This suggests that the TCD was responsible for the observed kinetics. Because norbornyl unsaturations are more reactive than cyclopentyl unsaturations and TCD solutions have a greater concentration of norbornyl double bonds than cyclopentyl double bonds, the reaction kinetics can be viewed as the initial fast polymerization through the norbornyl group with subsequent crosslinking at a slower rate. For DCPD polymerization, there is a 1:1 ratio of norbornyl to cyclopentyl unsaturations,

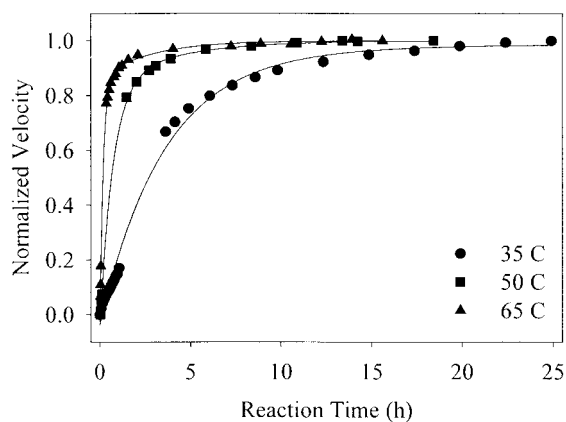


Figure 10. Change in the velocity during the polymerization of 15,000 mol of DCPD at different temperatures. The solid lines are the regressions of eq 9.

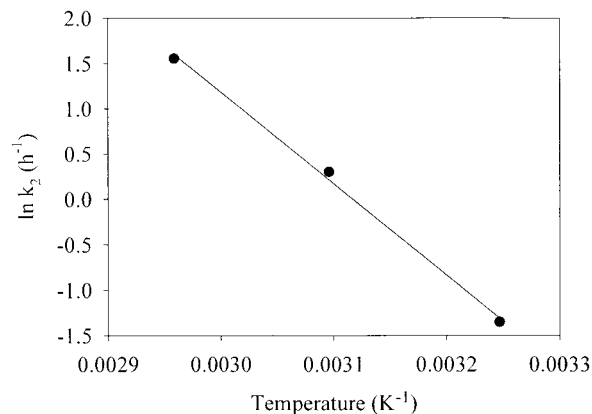


Figure 11. Arrhenius plot for the polymerization of 15,000 mol of DCPD with k_2 determined by ultrasonic velocity measurements and fitted with eq 9.

which suggests that gelation occurs earlier and that the reaction rate, as measured by ultrasound, is controlled by the reaction of the cyclopentyl unsaturation.

Temperature Effects

With an increasing reaction temperature, an increase in the rate of change of ultrasonic variables was observed (Fig. 10). Attenuation spectra also clearly illustrated that as the reaction temperature increased, the peak narrowed and moved to shorter reaction times. An Arrhenius plot was constructed for the crosslinking reaction from the velocity data fitted with eq 9 (Fig. 11). Both the velocity and modulus data led to similar linear Arrhenius plots, from which the activation energy was determined to be 84 kJ mol^{-1} with a pre-exponential factor of $7.21 \times 10^8 \text{ L mol}^{-1} \text{ s}^{-1}$. This shows that the Arrhenius behavior of the reaction could be followed by ultrasonic spectroscopy.

Frequency Effects

Ultrasound data obtained at different transducer frequencies exhibited the same concentration rate dependence as previously mentioned. As expected, the rate of the change of the sound velocity was independent of the transducer frequency. Although the modulus could be a frequency-dependent quantity, the ultimate modulus was independent of the transducer frequency. The modulus shifted to slightly lower values with an increasing transducer frequency (Fig. 12). The main observation from the frequency data was the time

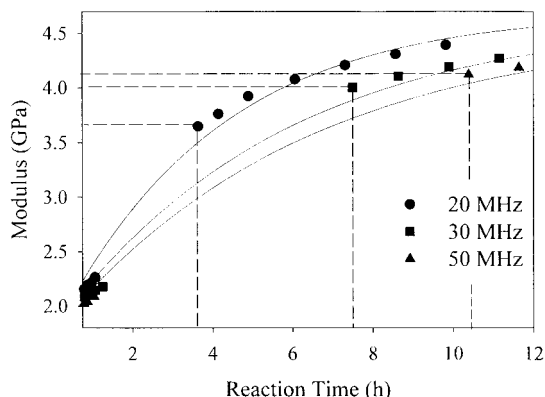


Figure 12. Acoustic modulus of the DCPD polymerization at vitrification as monitored with 20-, 30-, and 50-MHz transducers.

at which the signal returned after attenuation. Figure 13 displays the power spectra of the 20- and 50-MHz transducers at the initiation and final cure of DCPD. The change in attenuation during the polymerization was quite apparent, as was the shift in the frequency at the maximum amplitude. Each set of spectra showed a shift to lower frequencies, with a minimum occurring at the peak, that is, vitrification, in the attenuation, followed by partial recovery with continued curing. It was determined that there was no excess attenuation over the range of wavelengths characterized in this experiment, which would be indicative of scattering from heterogeneous domains. Therefore, the shift in the frequency and change in the duration of full attenuation were attributed to the medium's viscoelastic properties. The higher frequencies were more readily absorbed, requiring an increased level of cure (4.1 GPa at 50 MHz vs 3.6 GPa at 20 MHz) before full attenuation ceased. The frequency effects could further be modeled for a more quantitative analysis of the changes in the viscoelasticity.

CONCLUSIONS

Ultrasonic spectroscopy was used to monitor the reaction kinetics of the ROMP of DCPD. A reaction cell was constructed that allowed for accurate pulse echo scans of a polymerizing media. The reaction cell design allowed for the densification of the media to be measured during the polymerization. This, in turn, allowed for more accurate calculations of the sound velocity, acoustic modulus, and attenuation. Studies of the bulk polymer-

ization of DCPD by **1** at 25 °C revealed that the rate of densification was due to polymerization through the norbornyl double bond. Although FTIR monitored the polymerization of DCPD as two parallel reactions forming a common product, ultrasound only accurately monitored the crosslinking reaction. The rate constant for crosslinking calculated from the changes in the sound velocity and acoustic modulus agreed with that measured by FTIR when the ultrasound data were modeled with a rate equation for just the crosslinking reaction. For the copolymerization of DCPD with TCD, a rate dependence on the monomer concentration was discerned. This was not observed for the bulk polymerization of DCPD. The origin of the rate dependence was the stoichiometry of the norbornyl unsaturation to the cyclopentyl unsaturation and the different reaction rate of each functional group. By monitoring DCPD polymerizations at different temperatures, we confirmed the Arrhenius behavior of the crosslinking reaction. From the attenuation spectra, only qualitative information on the reaction rate could be obtained, as observed by the width and shift of the attenuation peak, but the point of vitrification could be determined. The effect of the frequency was apparent by an analysis of the attenuation spectra, in which the viscoelastic properties of the system absorbed the higher frequency sound waves, increasing the duration of full attenuation, so that an increased level of cure was needed to transmit the higher sound frequencies.

Financial support was provided by the Center for UMASS/Industry Research on Polymers. The authors

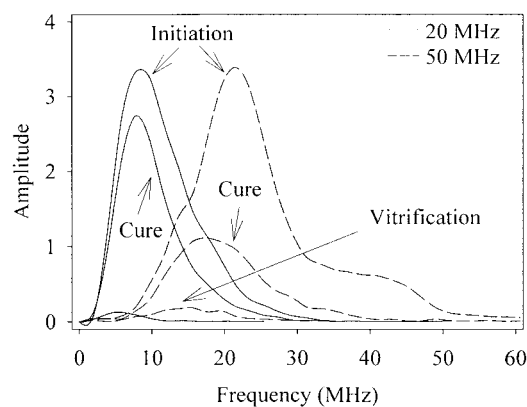


Figure 13. Power spectra at the initiation, vitrification, and cure of DCPD measured with 20- and 50-MHz transducers.

thank Donald Cotter for his assistance with the kinetic analysis.

REFERENCES AND NOTES

1. Encyclopedia of Chemical Technology; Howe-Grant, M., Ed.; Wiley-Interscience: New York, 1996; Volume 17, p 829.
2. Woodson, C. S.; Grubbs, R. H. (Advanced Polymer Technologies, Inc.). U.S. Patent 6,020,443, 2000.
3. Klosiewicz, D. W. (Hercules, Inc.). U.S. Patent 4,400,340, 1983.
4. Prime, R. B. In Thermal Characterization of Polymeric Materials; Turi, E. A., Ed.; Academic: New York, 1997; Chapter 2, pp 1380–1744.
5. Halley, P. J.; Mackay, M. E. *Polym Eng Sci* 1996, 36, 593–609.
6. Yang, Y. S.; Lee, L. J.; Lo, S. K. T.; Menardi, P. J. *J Appl Polym Sci* 1989, 37, 2313–2330.
7. Yang, Y. S.; Lafontaine, E.; Mortaigne, B. *Polymer* 1997, 38, 1121–1130.
8. Yang, Y. S.; Lafontaine, E.; Mortaigne, B. *J Appl Polym Sci* 1996, 60, 2419–2435.
9. Lindrose, A. M. *Exp Mech* 1978, 18, 227–232.
10. White, S. R.; Mather, P. T.; Smith, M. *J Polym Eng Sci* 2002, 42, 51–67.
11. Alig, I.; Nancke, K.; Johari, G. P. *J Polym Sci Part B: Polym Phys* 1994, 32, 1465–1474.
12. Schueneman, G. T. Ph.D. Thesis, University of Massachusetts, 1999.
13. Younes, M.; Wartewig, S.; Lellinger, D.; Strehmel, B.; Strehmel, V. *Polymer* 1994, 35, 5269–5278.
14. Osawa, E.; Tahara, Y.; Lizuka, T.; Tanaka, N.; Kan, T. *J Org Chem* 1982, 47, 1923–1932.
15. Dall'Asta, G.; Motroni, R.; Manetti, R.; Tosi, C. *Makromol Chem* 1969, 130, 153–165.
16. Nguyen, S. T.; Johnson, L. K.; Grubbs, R. H. *J Am Chem Soc* 1992, 114, 3974–3975.
17. Lynn, D. M.; Kanaoka, S.; Grubbs, R. H. *J Am Chem Soc* 1996, 118, 784–790.
18. Alig, I.; Lellinger, D.; Nancke, K.; Rizos, A.; Fytas, G. *J Appl Polym Sci* 1992, 44, 829–835.
19. Lee, C. C.; Lahham, M.; Martin, B. G. *IEEE Trans Ultrason Ferroelectr Freq Control* 1990, 37, 286–294.
20. Sanford, M. S.; Love, J. A.; Grubbs, R. H. *J Am Chem Soc* 2001, 123, 6543–6554.
21. Sanford, M. S.; Ulman, M.; Grubbs, R. H. *J Am Chem Soc* 2001, 123, 749–750.
22. Woodson, C. S.; Grubbs, R. H. (Advanced Polymer Technologies, Inc.). U.S. Patent 5,939,504, 1999.
23. Woodson, C. S.; Grubbs, R. H. (California Institute of Technology). U.S. Patent 5,728,785, 1998.
24. Encyclopedia of Chemical Technology; Howe-Grant, M., Ed.; Wiley-Interscience: New York, 1996; Volume 7, p 860.
25. Matsukawa, M.; Nagai, I. *J Acoust Soc Am* 1996, 99, 2110–2115.
26. Freemantle, R. J.; Challis, R. E. *Meas Sci Technol* 1998, 9, 1291–1302.